Distributed Consensus-Based Control of Multi-Quadcopter Systems for Formation Producing Under Cloud Access

Nargess Sadeghzadeh-Nokhodberiz, Allahyar Montazeri*

Abstract— **Large-scale cooperative environmental monitoring has introduced various challenges, such as intermittent links, power and bandwidth constraints, and interdicted inter-agent communication to the robotics community. Mobile cloud computing (MCC) has recently been introduced to tackle these problems, especially in the context of the formation control problem. Therefore, in this paper, the problem of formation producing control of multi-quadcopter systems under asynchronous access to the cloud is investigated. Here, it is assumed that the quadcopters exchange the information fully through the cloud storage service while the calculation for motion control is carried out on the edge. The scheduling rule is also designed to make cloud access more efficient without the need for constant communication. The formation producing is achieved by designing consensus-based control laws for the altitude and the translational subsystems while guaranteeing the asymptotic convergence of the quadcopters' positions to the biased average of the initial values. The results show that the modified controller after being applied through cloud access guarantees practical consensus with a calculated bounded error. The access to the could is achieved by designing a Zeno behavior-free scheduling rule.**

Formation control, Multi-quadcopter system, Mobile cloud computing, Consensus

I. Introduction

Autonomously operated quadcopters (quads) are vital for environmental monitoring due to their access to hazardous or unreachable areas [1], [2]. Given their resource limits (e.g., energy, computation, payload), cooperative multi-quad systems offer more efficient and reliable coverage of large areas [3]. However, cooperative control poses challenges due to intermittent wireless communication, especially over vast areas, leading to connectivity and power issues. Unlike traditional self-triggered methods, our approach reduces the need for constant inter-agent communication.

To reduce communication in multi-agent systems, event-triggered and protocol-based control strategies have been developed [4]–[6]. For instance, [7] introduces a finite-time, Zeno-free behavior event-triggered control scheme. *However, when quadrotors disperse over wide areas, peer-to-peer communication may become infeasible, limiting the applicability of such methods.* Recent works address this by relaxing connectivity constraints in sampled-data consensus [8] and formation control under limited-range communication [9]. Despite operating in a virtual communication layer, these methods increase onboard computational demands. Leveraging cloud services offers a more efficient trade-off between communication load and power consumption.

Mobile Cloud Computing (MCC), integrating mobile edge and cloud computing, addresses inter-agent communication limitations by enabling IoT devices—quadrotors in this study—to offload data to cloud servers for processing and storage [10], [11]. *However, in our study to retain the distributed nature of the solution, the cloud is used only for storage and as a pool of information shared by various agents.* The computational capacity of the agents is used to calculate the control laws and the scheduling times to access the cloud. *This architecture makes the system robust to a possible communication failure to the cloud by relying on local control laws.*

Formation control enables coordinated multi-quad operations in environmental monitoring, with distributed consensus-based methods favored for their scalability and effectiveness [12], [13]. Previous work like [14] addressed leaderless consensus for multi-quads using linearized models to manage nonlinear dynamics and under-actuation. *In contrast, we use full 6-DOF nonlinear dynamics from [1], ensuring formation via a bias-augmented consensus algorithm.* A hierarchical control approach handles under-actuation, as in [15].

In this framework, each quadrotor performs local processing at the edge while accessing shared data via a cloud service based on an individual connection schedule. This eliminates the need for continuous cloud communication and inter-agent messaging (for cases where inter-agent communication is impossible), enhancing scalability and reliability through a decentralized control strategy. The key challenge lies in maintaining formation control under asynchronous cloud access.

Previous studies, such as [16], investigated cloud-based formation control using asynchronous consensus for second-order systems via shared cloud storage. However, convergence to the average position only holds under zero initial velocities; otherwise, the system exhibits ramp behavior [17]. Similar limitations exist in [18], which extends to nonlinear systems but relies on first-order dynamics for analysis. Our recent work [19] advanced this framework to nonlinear 6-DOF underactuated quads, achieving practical consensus toward biased initial conditions. Nonetheless, the extended consensus filter still led to ramping under nonzero initial velocities. This work resolves that challenge effectively.

*Corresponding author: Allahyar Montazeri

Nargess Sadeghzadeh-Nokhodberiz is with the Department of Electrical and Computer Engineering, Qom University of Technology, Qom 3718146645, Iran e-mail: (sadeghzadeh@qut.ac.ir).

Allahyar Montazeri is with School of Engineering, Lancaster University, Lancaster, Lancashire, LA1 4YW, UK e-mail:(a.montazeri@lancaster.ac.uk)

This study addresses formation control in multi-quad systems with asynchronous cloud-based communication, where the cloud serves solely as shared storage and all processing occurs locally on each quad. A decentralized scheme is employed, with each agent using its own data and that of predefined neighbors to compute control laws. By distributing computation, the approach enhances scalability and reduces both cloud dependency and onboard computational load.

Elaborating further, The proposed approach first designs consensus-based formation control for the altitude subsystem, followed by translational control using virtual inputs. These controllers ensure asymptotic convergence to a biased average of initial positions. Adapted for cloud-based communication with scheduled access, the system achieves practical consensus with bounded error. Additionally, Zeno behavior is analyzed and shown to be avoided under the proposed scheduling scheme. The main novelties of the paper are specified in the following:
(1) A minor contribution is the design of consensus-based formation that produces control laws for altitude and translational subsystems using a hierarchical architecture and ensures convergence of the quad position to the biased average of initial values with asymptotic consensus.
(2) The major contribution is modifying controllers with cloud access, in which the practical consensus of the quad positions to the biased average of initial values is guaranteed through the design of a Zeno behavior-free scheduling rule.

This work advances prior cloud-based formation control studies [16], [19] by addressing key limitations. While [16] introduced the concept, it excludes nonlinear underactuated quadrotor dynamics. Although extended to 6-DOF quads in [19], that approach retains limitations due to the consensus filter employed. *In contrast, this paper employs a different, modified consensus filter adapted to ensure convergence to the biased average of initial positions.* Beyond that, new approximations and derivations are introduced across controller design, scheduling, and Zeno behavior analysis. *As shown in later sections, these enhancements simplify implementation, reduce computational load, and maintain strong performance.*

The paper is organized as follows. In Section II preliminaries are introduced. Consensus-based formation producing control for multi-quad systems is presented in Section III. Section IV extends the results to the formation producing control of multi-quad systems under cloud access. The simulation results are provided in Section V. Finally, Section VI concludes the paper.

II. Preliminaries

A. Multi-Quadcopter Architecture under Cloud Access

We consider a group of quadrotors communicating asynchronously via a cloud storage service, where each agent connects based on a predefined schedule and its data are only available during those intervals. As shown in Figure 1, this architecture eliminates the need for continuous cloud access and inter-agent communication, enabling efficient and scalable coordination.

The inter-agent communication is modeled as a predefined connectivity graph, where each quadrotor represents a node and edges denote communication links. This graph is stored in the cloud, enabling a publish/subscribe protocol: quads upload their data and download only that of designated neighbors. This cloud-mediated strategy eliminates peer-to-peer communication, reduces computational load, and supports a distributed control framework. While the fixed virtual graph ensures reliable operation even under intermittent cloud access, it limits adaptability in dynamically changing environments.

B. Graph Theory

Let $\mathcal{G} = (\mathcal{V}, \mathcal{E})$ be an undirected graph, representing the communication topology of the multi-quad system. $\mathcal{V} = \{\nu_1, \dots, \nu_N\}$ specifies the set of nodes and $\mathcal{E} \subseteq \mathcal{V} \times \mathcal{V}$ is the set of edges. Each edge is denoted by $e_{ij} = (\nu_i, \nu_j) \in \mathcal{E}$ where ν_i is known as the tail and ν_j as the head of the edge e_{ij}. The adjacency matrix $\mathcal{A} = [a_{ij}]$ of an undirected graphs is a matrix with non-zero elements such that $a_{ij} = 1$ if $(\nu_i, \nu_j) \in \mathcal{E}$ and $a_{ij} = 0$ otherwise. It is assumed that the size of $\mathcal{E}$ is M, that is $\mathcal{E} = \{E_1, \dots, E_M\}$ where $E_l = e_{ij}, l = 1, \dots M$. Besides, let $\mathcal{N}_i = \{\nu_j \in \mathcal{V} : a_{ij} \neq 0\}$ denote the set of neighbors of the node i. Let $\mathcal{L} \in \mathbb{R}^{N \times N}$ be the Laplacian matrix of the graph $\mathcal{G}$ which satisfies the $\mathcal{L} = BB^T$ with $B \in \mathbb{R}^{N \times M}$ is defined as the incidence matrix. This property holds regardless how the orientation of the graph $\mathcal{G}$ is chosen [20].
For a graph containing a spanning tree, the edge set is $\mathcal{T} \subseteq \mathcal{E} = \{E_1, \dots, E_{N-1}\}$ and $\mathcal{G} = \mathcal{G}_\mathcal{T} \cup \mathcal{G}_\mathcal{C}$ where $\mathcal{G}_\mathcal{T}$ is a given spanning tree and $\mathcal{G}_\mathcal{C}$ is the co-spanning tree. In this case, $B_\mathcal{T}$ is a full column rank minor of B, made up of the first $N-1$ columns of B. In other words, $B = [B_\mathcal{T} \; B_\mathcal{C}]$ where $B_\mathcal{T}$ and $B_\mathcal{C}$ are incidence matrices corresponding to $\mathcal{G}_\mathcal{T}$ and $\mathcal{G}_\mathcal{C}$. For such graphs, as $B_\mathcal{T}$ is full column rank, there exists an $(N-1) \times M$ matrix T such that the incidence matrix B can be written as $B = B_\mathcal{T} T$ which results in $T = (B_\mathcal{T}^\mathrm{T} B_\mathcal{T})^{-1} B_\mathcal{T}^\mathrm{T} B$. Therefore, $\mathcal{L} = BB^\mathrm{T} = B_\mathcal{T} T T^\mathrm{T} B_\mathcal{T}^\mathrm{T}$ [16], [21].
It is also worth mentioning that the graph $\mathcal{G}$ is connected if and only if $rank(\mathcal{L}) = N - 1$. In other words, a graph is called connected if a path between any two distinct nodes of the graph can be found. Moreover, in $\mathcal{L}$ sums of all the rows are zero and thus $\mathbf{1}_N = [1, 1, \dots, 1]^T \in \mathbb{R}^N$ is an eigenvector of $\mathcal{L}$ associated with the eigenvalue $\lambda = 0$. [22], [23].

C. Consensus Control for Agents with Double-Integrator Dynamics

Given a graph $\mathcal{G}$, let $q_{1i}(t) \in \mathcal{R}$ and $q_{2i}(t) \in \mathcal{R}$ denote the states of node ν_i at time instant $t \in \mathcal{R}_+$. Besides, each node i of the graph is a dynamic agent with the following double-integrator dynamics:

$$\dot{q}_{1i}(t) = q_{2i}(t), \; \dot{q}_{2i}(t) = u_i(t), \tag{1}$$

where $u_i(t)$ is the control input of the i-th agent and the collective initial condition vectors are defined as $q_1(0) = [q_{11}(0), q_{12}(0), \dots, q_{1N}(0)]^\mathrm{T}$, $q_2(0) = [q_{21}(0), q_{22}(0), \dots, q_{2N}(0)]^\mathrm{T}$.

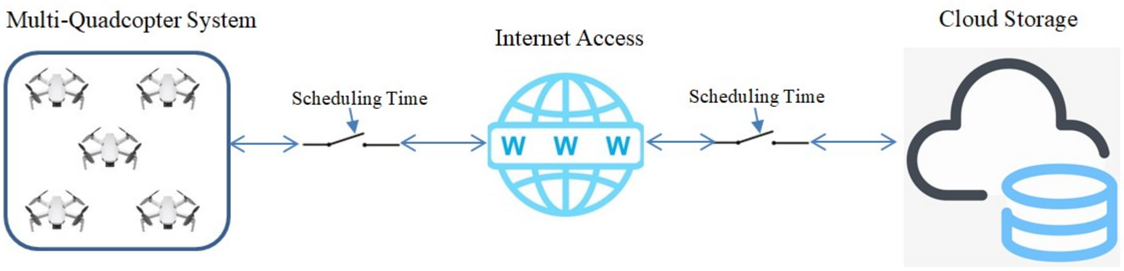

Fig. 1: A multi-quadcopter system communicating through a cloud access.

The control input $u_i(t)$ is designed by considering the following consensus control protocol for each agent:

$$u_i(t) = \sum_{j\in\mathcal{N}_i} (q_{1j}(t) - q_{1i}(t)) + kq_{2i}(t), \tag{2}$$

where $k < 0$ is a negative feedback gain.
As proven in [24], for a network of dynamic agents with the dynamics presented in (1) and a connected fixed graph topology $\mathcal{G}$, under the control protocol (2), $q_{1i}(t)$ and $q_{2i}(t)$ for $i = 1, \dots, N$ globally asymptotically converge to the following values:

$$\lim_{t\to\infty} q_{1i}(t) = \frac{1}{N}\sum_{j=1}^{N}\big(q_{1j}(0) - \frac{q_{2j}(0)}{k}\big), \ \lim_{t\to\infty} q_{2i}(t) = 0. \tag{3}$$

It is obvious that the presented distributed control protocol (2) solves *average consensus* problem if $q_{2i}(0) = 0, i = 1, \dots N$ [24].

D. State Space Model of Multi-Quadcopter System

According to Figure 1, consider N quadcopters communicating with each other through cloud access in which each quadcopter uploads its own information and downloads the information from some other quads in the neighborhood at each time instant. In this way, it is assumed that the group of quadcopters constructs a connected undirected connectivity graph. For consistency in the paper, the index i is used to refer to the parameters of the i-th quadcopter. Therefore, the state space model of a multi-quadcopter system can be presented as follows [25]. It is worth mentioning that for the sake of brevity and to avoid similarity, the readers are referenced to [25] for the exact non-linear 6-DOF model of the quadcopter.

1) Altitude Subsystem: The altitude subsystem (position in z-axis) can be written in the form of continuous-time state space model for the i-th agent as follows:

$$\dot{x}_{1i}(t) = x_{2i}(t), \ \dot{x}_{2i}(t) = -g + \gamma_{2i}(t)u_{1i}(t), \tag{4}$$

where g is the gravitational constant, $x_{1i}(t) = z_i(t)$ and $x_{2i}(t) = \dot{z}_i(t)$ are the i-th quadcopter's altitude and speed in the inertial frame, respectively. In (4), $\gamma_{2i}(t) = \frac{\cos(\phi_i(t))\cos(\theta_i(t))}{m_i}$ with $\phi_i(t)$ and $\theta_i(t)$ are defined as the roll and pitch angles of the quad. Besides, $u_{1i}(t)$ defines the main thrust created by the combined forces of the rotors. Now, assuming that $X_1(t) = [x_{11}(t) \ \dots \ x_{1N}(t)]^T$, $X_2(t) = [x_{21}(t) \ \dots \ x_{2N}(t)]^T$, and $U_1(t) = [u_{11}(t) \ \dots \ u_{1N}(t)]^T$, the following collective state space model for the altitude subsystem can be written :

$$\dot{X}_1(t) = X_2(t), \dot{X}_2(t) = -G + \Gamma_2(t)U_1(t), \tag{5}$$

where $G = g\mathbf{1}_N$, and $\Gamma_2(t) = \mathrm{diag}[\gamma_{21}(t) \dots \gamma_{2N}(t)]$.

2) Translational Subsystem: Due to the under-actuated nature of the position subsystem in the quadcopter's dynamics, we define two virtual inputs as $u_{xi}(t) = \cos(\psi_i(t))\sin(\theta_i(t))\cos(\phi_i(t)) + \sin(\psi_i(t))\sin(\phi_i(t))$ and $u_{yi}(t) = \sin(\psi_i(t))\sin(\theta_i(t))\cos(\phi_i(t)) - \cos(\psi_i(t))\sin(\phi_i(t))$ where $\psi_i(t)$ is the yaw angle. The state space model of the translational subsystem for the i-th subsystem can be formulated as:

$$\dot{x}_{3i}(t) = x_{4i}(t), \ \dot{x}_{4i}(t) = \gamma_{4i}(t)u_{vi}(t), \tag{6}$$

where $x_{3i}(t) = [x_i(t) \ y_i(t)]^{\mathrm{T}}$ and $x_{4i}(t) = [\dot{x}_i(t) \ \dot{y}_i(t)]^{\mathrm{T}}$ are the position and velocity vectors of the i-th quadcopter in 2D (x-y plane) in the inertial frame. In (6), $u_{vi}(t) = [u_{xi}(t) \ u_{yi}(t)]^{\mathrm{T}}$ and $\gamma_{4i}(t) = \frac{u_{1i}(t)}{m_i}$. Therefore, the collective state-space model of the translational subsystem can be formulated as:

$$\dot{X}_3(t) = X_4(t), \ \dot{X}_4(t) = \big(\Gamma_4(t) \otimes \mathrm{I}_2\big)U_v(t), \tag{7}$$

where $\otimes$ refers to the Krnonecker product, $X_3(t) = [x_{31}^{\mathrm{T}}(t), \dots, x_{3N}^{\mathrm{T}}(t)]^{\mathrm{T}}$, $X_4 = [x_{41}^{\mathrm{T}}(t), \dots, x_{4N}^{\mathrm{T}}(t)]^{\mathrm{T}}$, $U_v(t) = [u_{v1}^{\mathrm{T}}(t), \dots, u_{vN}^{\mathrm{T}}(t)]^{\mathrm{T}}$, and $\Gamma_4(t) = \mathrm{diag}[\gamma_{41}(t) \dots \gamma_{4N}(t)]$.

Remark 1: Since during the maneuver the rotors never turn off and at least a thrust should be generated for hovering, one can conclude that $u_{1i}(t) \neq 0, \forall t \geq 0$.

III. Consensus Based Formation Producing Control For Multi-Quadcopter System

In this section, a formation producing control policy is designed for the multi-quadcopter system formulated in the previous section. For this, we use the state space model of the position subsystem presented in II-D and the consensus control policy defined for agents with double-integrator dynamics in II-C.

A. Assumptions

To design consensus-based control and ensure convergence under cloud access, the following assumptions are adopted as part of the modeling and control development process.

Assumption 1: (Zero Initial Velocities) all quadcopters start with zero velocity in each degree of freedom, i.e., $\dot{x}_i(t) = \dot{y}_i(t) = \dot{z}_i(t) = 0, \forall i = 1, \dots N$.

Assumption 2: (Cloud Storage Model) the cloud server acts as a shared storage repository, and each quadcopter uploads its own state and downloads the latest available data from its predefined neighbors. There is no direct peer-to-peer communication.

Assumption 3: (Fixed Communication Graph) the inter-agent communication topology is modeled as a connected undirected graph stored in the cloud. The set of neighbors is predefined and does not change dynamically.

Assumption 4: (Containing Spanning Tree) The multi-quadcopter system network graph $\mathcal{G}$ contains a spanning tree.

Assumption 5: (Nonzero Thrust) the thrust input $u_{1i}(t) \neq 0$ at all times $t \geq 0$.

Remark 2: while some assumptions simplify the analysis, they reflect realistic constraints for quadcopters operating in structured missions (e.g., aerial surveying or environmental monitoring). The assumptions are integrated into the control procedure and are clearly referenced where required.

B. Consensus Based Control Law

The control objective is to shape a formation for the agents defined by the bias vectors $b_1, \dots, b_N$ where $b_i = [b_{zi}\ b_{xi}\ b_{yi}]^{\mathrm{T}}$ for $i = 1, \dots, N$. Here it is assumed that the biases are stored in the cloud and can be downloaded at the scheduling time to the quad for control law calculations.

For the multi-quadcopter system with the agent-wise dynamics presented in (4) and (6) consider the following consensus-type control protocols:

$$u_{1i}(t) = \gamma_{2i}^{-1}(t)\big(g - \sum_{j \in \mathcal{N}_i} (x_{1i}(t) - b_{zi} - x_{1j}(t) + b_{zj}) - x_{2i}(t)\big), \tag{8}$$

and

$$u_{vi}(t) = -\gamma_{4i}^{-1}(t)\big(\sum_{j \in \mathcal{N}_i} (x_{3i}(t) - b_{3i} - x_{3j}(t) + b_{3j}) - x_{4i}(t)\big), \tag{9}$$

with $b_{3i} = [b_{xi}\ b_{yi}]^{\mathrm{T}}$ and assuming that the initial speed of each quadcopter is zero, i.e. $\dot{x}_i(0) = \dot{y}_i(0) = \dot{z}_i(0) = 0, i = 1 \dots N$.

Remark 3: The control of quadcopter's altitude in the singular orientation of $\cos(\phi_i(t))\cos(\theta_i(t)) = 0$ is not possible and this is avoided in practice. Otherwise, according to (8), $u_{1i}(t) \rightarrow \infty$ and since $\gamma_{4i}(t) = \frac{u_{1i}(t)}{m_i}$ and according to (9), $u_{vi}(t) \rightarrow 0$ which gives $u_{xi}(t) \rightarrow 0$ and $u_{yi}(t) \rightarrow 0$. Therefore, according to [25], $\sin(\phi_i(t)) = u_{xi}(t)\sin(\psi_i(t)) - u_{yi}(t)\cos(\psi_i(t))$ and $\sin(\theta_i(t)) = \frac{u_{xi}(t)\sin(\psi_i(t)) + u_{yi}(t)\sin(\psi_i(t))}{\cos(\phi_i(t)}$, one can conclude $\sin(\phi_i(t)) = 0$ and $\sin(\theta_i(t)) = 0$ which contradicts $\cos(\phi_i(t))\cos(\theta_i(t)) = 0$.
Besides, let $x'_{1i}(t) := x_{1i}(t) - b_{zi}$ and therefore first equation in (4) changes to $\dot{x}'_{1i}(t) = x_{2i}(t)$. Now, rewrite (8) as $u_{1i}(t) = \gamma_{2i}^{-1}(t)\big(g + u'_{1i}(t)\big)$ where

$$u'_{1i}(t) = \sum_{j \in \mathcal{N}_i} (x'_{1j}(t) - x'_{1i}(t)) - x_{2i}(t). \tag{10}$$

By replacing $u_{1i}(t)$ in (4) we will have:

$$\dot{x}'_{1i}(t) = x_{2i}(t),\ \dot{x}_{2i}(t) = u'_{1i}(t). \tag{11}$$

Comparing (11) and (10) with (1) and (2) and using (3), one can conclude that $\lim_{t\to\infty} x'_{1i}(t) = \bar{x}'_1(0) - \bar{x}_2(0)$ and $\lim_{t\to\infty} x_{2i}(t) = 0$ where $\bar{.}$ refers to averaging on N agents. Considering $\bar{x}_2(0) = 0$, the global asymptotic convergence of $x_{1i}(t)$ to average of the initial positions with the biased term of $b'_{zi} = b_{zi} - \bar{b}_{zi}$ is guaranteed.
Now, by defining $x'_{3i}(t) := x_{3i}(t) - b_{3i}(t)$ and substituting in (6), the first equation changes to $\dot{x}'_{3i}(t) = x_{4i}(t)$. Now, let

$$u'_{vi}(t) = \sum_{j \in \mathcal{N}_i} (x'_{3j}(t) - x'_{3i}(t)) - x_{4i}(t). \tag{12}$$

According to (9) $u_{vi} = \gamma_{4i}^{-1}(t)u'_{vi}(t)$, and by replacing this form of u_{vi} in (6) one can conclude:

$$\dot{x}'_{3i}(t) = x_{4i}(t),\ \dot{x}_{4i}(t) = u'_{vi}(t). \tag{13}$$

Now by element-wise comparison of (13) and (12) with (1) and (2), it can be concluded from (3) that $\lim_{t\to\infty} x'_{3i}(t) = \bar{x}'_3(0) - \bar{x}_4(0)$ and $\lim_{t\to\infty} x_{4i}(t) = \mathbf{0}_2$. Since $\bar{x}_4(0) = \mathbf{0}_2$, the global asymptotic convergence of $x_{3i}(t)$ to the average of its initial values with biased term of $[b'_{xi} b'_{yi}]^{\mathrm{T}}$ with $b'_{xi} = b_{xi} - \bar{b}_{xi}$, $b'_{yi} = b_{yi} - \bar{b}_{yi}$ can be concluded.

IV. Consensus Based Formation Producing Control For Multi-Quadcopter System Under Cloud Access

In this section, the data transmission scenario between the agents under the cloud access is explained first. Then, the proposed controllers in (8) and (9) are modified, such that the formation producing is guaranteed under some bounds on the input errors. A cloud access scheduling rule is then designed to guarantee boundedness of the input error. Then, it is shown that the sequence of cloud access times does not present a Zeno behavior.

A. Cloud Access Data Transmission Scenario

As mentioned previously, in Subsection II-A, the agents are communicating with each other through the cloud repository. For this purpose, they upload their information containing their altitude and translational states, as well as their control laws and simultaneously download the latest information of their neighboring agents. Let $t_{i,k}$ be the k-th time instant that the i-th agent accesses the cloud. Then, the latest access of the neighboring agent $j \in \mathcal{N}_i$ is shown by $t_{j,f_j(t_{i,k})}$. In other words, according to [16], $f_j(t) = \max\{l \in \mathbb{N} : t_{j,l} \leq t\}$. When i-th agent is connected to the cloud the set $D_{t_{i,k}} = \big\{x_{1i}(t_{i,k}), x_{2i}(t_{i,k}), x_{3i}(t_{i,k}), x_{4i}(t_{i,k}), u_{1i}(t_{i,k}), u_{vi}(t_{i,k})\big\}$ is uploaded and the set $D_{t_{j,f_j(t_{i,k})}} = \big\{x_{1j}(t_{j,f_j(t_{i,k})}), x_{2j}(t_{j,f_j(t_{i,k})}), x_{3j}(t_{j,f_j(t_{i,k})}), x_{4j}(t_{j,f_j(t_{i,k})}), u_{1j}(t_{j,f_j(t_{i,k})}), u_{vj}(t_{j,f_j(t_{i,k})}), b_j, b_i\big\}, j \in \mathcal{N}_i$, is downloaded

Remark 4: To save the energy and computational burden on the quad, it is possible to read the values sensed by the GPS only at the scheduling times when the quad is connected to the cloud. In other words, the synthesis of the control law requires only access to $x_{1i}(t_{i,k}), x_{2i}(t_{i,k}), x_{3i}(t_{i,k}), x_{4i}(t_{i,k})$ during the time interval $[t_{i,k}\ t_{i,k+1})$. However, the quad should rely on continuous reading of GPS and other on-board data when it is not connected to the cloud due to lack of internet or disruption.

B. The Controller Under Cloud Access

By following the cloud access scenario presented just now, since the value of $x'_{1j}(t_{i,k})$ is not available at time instant $t_{i,k}$, the controller in (8) is replaced by the following controller for $t \in [t_{i,k}\ t_{i,k+1})$:

$$u_{1i,k}(t) = \gamma_{2i}^{-1}(t)\big(g - \sum_{j\in\mathcal{N}_i}(\hat{x}'_{1j}(t_{i,k}) - x'_{1i}(t_{i,k})) - x_{2i}(t_{i,k})\big), \tag{14}$$

where $\hat{x}'_{1j}(t_{i,k})$ is an estimate of $x'_{1j}(t_{i,k})$ using the system dynamics in (11) as follows:

$$\hat{x}'_{1j}(t_{i,k}) = x'_{1j}(t_{j,f_j(t_{i,k})}) + (t_{i,k} - t_{j,f_j(t_{i,k})})x_{2j}(t_{j,f_j(t_{i,k})}). \tag{15}$$

Similarly, the controller in (9) is replaced with the following one for $t \in [t_{i,k}\ t_{i,k+1})$:

$$u_{vi,k}(t) = -\gamma_{4i}^{-1}(t)\big(\sum_{j\in\mathcal{N}_i}(\hat{x}'_{3j}(t_{i,k}) - x'_{3i}(t_{i,k})) - x_{4i}(t_{i,k})\big), \tag{16}$$

where $\hat{x}'_{3j}(t_{i,k})$ is estimated using (13) as follows:

$$\hat{x}'_{3j}(t_{i,k}) = x'_{3j}(t_{j,f_j(t_{i,k})}) + (t_{i,k} - t_{j,f_j(t_{i,k})})x_{4j}(t_{j,f_j(t_{i,k})}). \tag{17}$$

Remark 5: When $u_{1i,k}(t)$ is applied to the system instead of $u_{1i}(t)$, $\gamma_{4i}(t) = \frac{u_{1i}(t)}{m_i}$ should be replaced with $\gamma_{4i,k}(t) = \frac{u_{1i,k}(t)}{m_i}$. However, to reduce the complexity $\gamma_{4i,k}(t)$ is approximated with $\gamma_{4i}(t)$ in the rest of this paper.

Now, let us define the difference between the desired controllers $u_{1i}(t)$ and $u_{vi}(t)$ and the ones proposed under cloud access $u_{1i,k}(t)$ and $u_{vi,k}(t)$, respectively, as follows:

$$\tilde{u}_{1i}(t) = u_{1i,k}(t) - u_{1i}(t),\ \tilde{u}_{vi}(t) = u_{vi,k}(t) - u_{vi}(t). \tag{18}$$

Now, assuming that $U_{1,k}(t) = [u_{11,k}, \ldots, u_{1N,k}]^{\mathrm{T}}$ and $U_{v,k}(t) = [u_{v1,k}^{\mathrm{T}}, \ldots, u_{vN,k}^{\mathrm{T}}]^{\mathrm{T}}$, we can write $U_{1,k}(t) = \tilde{U}_{1,k}(t) + U_1(t)$ and $U_{v,k}(t) = \tilde{U}_{v,k}(t) + U_v(t)$, where $\tilde{U}_1(t) = [\tilde{u}_{11}(t), \ldots, \tilde{u}_{1N}(t)]^{\mathrm{T}}$ and $\tilde{U}_v(t) = [\tilde{u}_{v1}^{\mathrm{T}}(t), \ldots, \tilde{u}_{vN}^{\mathrm{T}}(t)]^{\mathrm{T}}$. Now according to (10), it can be concluded that $U_1(t) = \Gamma_2^{-1}(t)\big(G - \mathcal{L}X'_1(t) - X_2(t)\big)$, where $X'_1 = [x'_{11}, \ldots, x'_{1N}]^{\mathrm{T}}$ and $X_2 = [x_{21}, \ldots, x_{2N}]^{\mathrm{T}}$. Replacing $U_{1,k}(t) = \tilde{U}_{1,k}(t) + \Gamma_2^{-1}(t)\big(G - \mathcal{L}X'_1(t) - X_2(t)\big)$ in (5), the following is obtained:

$$\begin{aligned}\dot{X}'_1(t) &= X_2(t),\\ \dot{X}_2(t) &= -\mathcal{L}X'_1(t) - X_2(t) + \Gamma_2(t)\tilde{U}_{1,k}(t).\end{aligned} \tag{19}$$

In addition, following (12), $U_v(t) = -\Gamma_4^{-1}\big(\big(\mathcal{L}\otimes \mathrm{I}_2\big)X'_3(t) - X_4(t)\big)$, where $X'_3 = [x'^{\mathrm{T}}_{31}, \ldots, x'^{\mathrm{T}}_{3N}]^{\mathrm{T}}$, $X_4 = [x^{\mathrm{T}}_{41}, \ldots, x^{\mathrm{T}}_{4N}]^{\mathrm{T}}$. Thus, if $U_{v,k}(t) = U_v(t) + \tilde{U}_{v,k}(t)$ is replaced in (7), the following expression is achieved:

$$\begin{aligned}&\dot{X}'_3(t) = X_4(t),\\ &\dot{X}_4(t) = -\big(\mathcal{L}\otimes \mathrm{I}_2\big)X'_1(t) - X_4(t) + \big(\Gamma_4(t)\otimes \mathrm{I}_2\big)\tilde{U}_{v,k}(t).\end{aligned} \tag{20}$$

Now, define the collective edge states [16] of the multi-quadcopter system as $X''_1 := B_{\mathcal{T}}^{T}X'_1$, $X''_2 := B_{\mathcal{T}}^{T}X_2$, $X''_3 := (B_{\mathcal{T}}^{T}\otimes \mathbf{I}_2)X'_3$, and $X''_4 := (B_{\mathcal{T}}^{T}\otimes \mathbf{I}_2)X_4$.

From Section III, it can be proven that $\lim_{t\to\infty}\|\xi_1\| = 0$ and $\lim_{t\to\infty}\|\xi_3\| = 0$, where $\xi_1 = [X''^{\mathrm{T}}_1\ X''^{\mathrm{T}}_2]^{\mathrm{T}}$ and $\xi_3 = [X''^{\mathrm{T}}_3\ X''^{\mathrm{T}}_4]^{\mathrm{T}}$. In this case, the system with the states ξ_1 and ξ_3 can reach an asymptotic consensus over the graph $\mathcal{G}$.

Remark 6: It is worth mentioning that during this paper $\|.\|$ refers to norm 2 of the matrix or vector.

Definition 1: The multi-quadcopter system achieves practical consensus [16] on $\mathcal{G}$ if there exist $\mathcal{X}_1 \geq 0$ and $\mathcal{X}_3 \geq 0$ such that $\lim_{t\to\infty}\|\xi_1\| \leq \mathcal{X}_1$ and $\lim_{t\to\infty}\|\xi_3\| \leq \mathcal{X}_3$.

Theorem 1: **(Practical Consensus under Cloud Access)** The multi-quadcopter system with the state space model presented in (5) and (7) under the cloud access data transmission scenario presented in subsection IV-A and with the controllers proposed in (14) and (16) **achieves the practical consensus** with $\mathcal{X}_1$ and $\mathcal{X}_3$ defined according to (21) and (22), if $|\tilde{u}_{1i}| < \zeta_1$ and $\|\tilde{u}_{vi}\| < \zeta_3$ for $i = 1, \ldots, N$.

$$\mathcal{X}_1 = \zeta_1\sqrt{N}\frac{\|B_{\mathcal{T}}\|}{\lambda_{max1}m_{min}}, \tag{21}$$

where $\lambda_{max1} = -\max\{\Re(\lambda_{F_1}) : \lambda_{F_1} \in \mathrm{eig}(F_1)\}$ (where $F_1 = \begin{bmatrix}\mathbf{0}_{(N-1)\times(N-1)} & \mathbf{I}_{N-1}\\ -B_{\mathcal{T}}^{\mathrm{T}}BT^{\mathrm{T}} & -\mathbf{I}_{N-1}\end{bmatrix}$ and F_1 is Hurwitz (see Appendix I for the proof) and m_{min} is the minimum weight of the quadcopters. Besides

$$\mathcal{X}_3 = \zeta_3\sqrt{N}\|B_{\mathcal{T}}\|\frac{u_{1max}}{\lambda_{max3}m_{min}}, \tag{22}$$

where $\lambda_{max3} = -\max\{\Re(\lambda_{F_3}) : \lambda_{F_3} \in \mathrm{eig}(F_3)\}$ (where $F_3 = \begin{bmatrix}\mathbf{0}_{(2N-2)\times(2N-2)} & \mathbf{I}_{2N-2}\\ -\big(B_{\mathcal{T}}^{\mathrm{T}}BT^{\mathrm{T}}\otimes \mathrm{I}_2\big) & -\mathbf{I}_{2N-2}\end{bmatrix}$ and F_3 is Hurwitz (see Appendix II for the proof) and $u_{1i}(t) \leq u_{1max}$ (see Appendix III for the proof).

Proof: We consider the altitude subsystem with the collective dynamical model presented in (19). Multiplying the model by $B_{\mathcal{T}}^{\mathrm{T}}$ from left hand side, the state space model of the system can be written in terms of the edge states $X''_1(t)$ and $X''_2(t)$:

$$\begin{aligned}\dot{X}''_1(t) &= X''_2(t),\\ \dot{X}''_2(t) &= -B_{\mathcal{T}}^{\mathrm{T}}BT^{\mathrm{T}}X''_1(t) - X''_2(t) + B_{\mathcal{T}}^{\mathrm{T}}\Gamma_2(t)\tilde{U}_1(t).\end{aligned} \tag{23}$$

Therefore,

$$\dot{\xi}_1(t) = F_1\xi_1(t) + H_1(t)\tilde{U}_1(t), \tag{24}$$

where $H_1(t) = [\mathbf{0}_N^{\mathrm{T}}\ \Gamma_2(t)B_{\mathcal{T}}]^{\mathrm{T}}$. The solution of (24) is

$$\xi_1(t) = e^{F_1 t}\xi_1(0) + \int_0^t e^{F_1(t-\tau)}H_1(\tau)\tilde{U}_1(\tau)d\tau. \qquad (25)$$

Applying the triangular inequality to (25) and knowing that $\|e^{F_1(t-\tau)}\| \leq e^{-\lambda_{max1}(t-\tau)}$ [26], $\|H_1\| = \|\Gamma_2(t)\|\|B_{\mathcal{T}}\| \leq \frac{\|B_{\mathcal{T}}\|}{m_{min}}$, and $\|\xi_1(0)\| \leq \xi_{10}$ it can be concluded:

$$\|\xi_1(t)\| \leq e^{-\lambda_{max1}t}\xi_{10} + \zeta_1\sqrt{N}\frac{\|B_{\mathcal{T}}\|}{m_{min}}\int_0^t e^{-\lambda_{max1}(t-\tau)}d\tau. \qquad (26)$$

Therefore, $\lim\limits_{t\to\infty}\|\xi_1\| \leq \mathcal{X}_1$ with $\mathcal{X}_1$ presented in (21).

For the translational subsystem we consider the collective dynamical model presented in (20).

Remark 7: If A, B, C and D are matrices of such size that one can form the matrix products AC and BD then $(A\otimes B)(C\otimes D) = (AC)\otimes(BD)$. This property is called the mixed product property [27].

Multiplying the model by $B_{\mathcal{T}}^{\mathrm{T}} \otimes \mathbf{I}_2$ from left side and using Remark 7, the state space model below in terms of the edge states $X_3''(t)$ and $X_4''(t)$ can be achieved:

$$\begin{aligned}\dot{X}_3''(t) =& X_4''(t),\\ \dot{X}_4''(t) =& -\big(B_{\mathcal{T}}^{\mathrm{T}}BT^{\mathrm{T}} \otimes \mathrm{I}_2\big)X_3''(t) - X_4''(t)\\ &+ \big(B_{\mathcal{T}}^{\mathrm{T}}\Gamma_4(t) \otimes \mathrm{I}_2\big)\tilde{U}_v(t).\end{aligned} \qquad (27)$$

In deriving (27), this equality $\big(B_{\mathcal{T}}^{\mathrm{T}}\otimes\mathbf{I}_2\big)\big(\mathcal{L}\otimes\mathrm{I}_2\big) = \big(B_{\mathcal{T}}^{\mathrm{T}}\mathcal{L}\otimes\mathbf{I}_2\big)$ is used, following Remark 7. Now, by substituting $\mathcal{L} = BB^{\mathrm{T}} = BT^{\mathrm{T}}B_{\mathcal{T}}^{\mathrm{T}}$ and using Remark 7 it can be readily concluded that $\big(B_{\mathcal{T}}^{\mathrm{T}}\mathcal{L}\otimes\mathbf{I}_2\big) = \big(B_{\mathcal{T}}^{\mathrm{T}}BT^{\mathrm{T}}B_{\mathcal{T}}^{\mathrm{T}}\otimes\mathbf{I}_2\big) = \big(B_{\mathcal{T}}^{\mathrm{T}}BT^{\mathrm{T}}\otimes \mathbf{I}_2\big)\big(B_{\mathcal{T}}^{\mathrm{T}}\otimes\mathbf{I}_2\big)$.

As such

$$\dot{\xi}_3(t) = F_3\xi_3(t) + H_3(t)\tilde{U}_v(t), \qquad (28)$$

where $H_3(t) = [\mathbf{0}_{2N}^{\mathrm{T}}\ \big(B_{\mathcal{T}}^{\mathrm{T}}\Gamma_4(t)\otimes\mathrm{I}_2\big)^{\mathrm{T}}]^{\mathrm{T}}$. The solution of (28) can be written as:

$$\xi_3(t) = e^{F_3 t}\xi_3(0) + \int_0^t e^{F_3(t-\tau)}H_3(\tau)\tilde{U}_v(\tau)d\tau. \qquad (29)$$

Applying the triangular inequality to (29) and knowing that $\|e^{F_3(t-\tau)}\| \leq e^{-\lambda_{max3}(t-\tau)}$ [26], $\|H_3\| = \|\Gamma_4(t)\|\|B_{\mathcal{T}}\| \leq \frac{u_{1max}\|B_{\mathcal{T}}\|}{m_{min}}$, and $\|\xi_3(0)\| \leq \xi_{30}$ the following inequality can be achieved:

$$\|\xi_3(t)\| \leq e^{-\lambda_{max3}t}\xi_{30}+\zeta_3\sqrt{N}\|B_{\mathcal{T}}\|\frac{u_{1max}}{m_{min}}\int_0^t e^{-\lambda_{max3}(t-\tau)}d\tau. \qquad (30)$$

As such $\lim\limits_{t\to\infty}\|\xi_3\| \leq \mathcal{X}_3$ with $\mathcal{X}_3$ presented in (22). ■

Remark 8: Parameters ζ_1 and ζ_3 can be selected with purpose. Toward this, according to Definition 1, some desired upper bounds ($\mathcal{X}_1$ and $\mathcal{X}_3$) can be selected approximately for the norms of the edge states because $\|\xi_1\| \leq \mathcal{X}_1$ and $\|\xi_3\| \leq \mathcal{X}_3$). Therefore, according to (21) and (22), the values of ζ_1 and ζ_3 can be determined approximately.

C. The Scheduling Rule For The Cloud Access

As mentioned in Theorem 1, if $|\tilde{u}_{1i}| < \zeta_1$ and $\|\tilde{u}_{vi}\| < \zeta_3$ for $i = 1,\dots,N$, the controllers proposed in (14) and (16) solve the practical consensus. In this subsection, the main goal is to find a scheduling rule under which $|\tilde{u}_{1i}| < \zeta_1$ and $\|\tilde{u}_{vi}\| < \zeta_3$ hold for $i = 1,\dots,N$. In addition, it is also concluded that the sequence of cloud access update times does not show Zeno behavior.

Theorem 2: **(Zeno-Free Cloud Scheduling)** Consider the multi-quadcopter system with the state space model presented in (5) and (7), the cloud access data transmission scenario presented in Subsection IV-A, the control laws (14) and (16), and the scheduling rule in (31), it is guaranteed that $|\tilde{u}_{1i}| < \zeta_1$ and $\|\tilde{u}_{vi}\| < \zeta_3$ for $i = 1,\dots,N$.

$$t_{i,k+1} = \min\{\frac{\zeta_1 + |A_{1i}|t_{i,k}}{|A_{1i}|}, \frac{\zeta_3 + \|A_{3i}\|t_{i,k}}{\|A_{3i}\|}\}, k \in \mathbb{N} \qquad (31)$$

where

$$\begin{aligned}A_{1i} = \gamma_{2i}^{-1}(t_{i,k})\big((N_i-1)x_{2i}(t_{i,k}) - N_i x_{1i}'(t_{i,k})+\\ \sum_{j\in\mathcal{N}_i}(\hat{x}_{1j}'(t_{k,i}) - \hat{x}_{2j}(t_{k,i}))\big),\end{aligned} \qquad (32)$$

and

$$\begin{aligned}A_{3i} = \gamma_{4i}^{-1}(t_{i,k})\big((N_i-1)x_{4i}(t_{i,k}) - N_i x_{3i}'(t_{i,k})+\\ \sum_{j\in\mathcal{N}_i}(\hat{x}_{3j}'(t_{k,i}) - \hat{x}_{4j}(t_{k,i}))\big),\end{aligned} \qquad (33)$$

where $N_i = |\mathcal{N}_i|$, $\hat{x}_{1j}'(t_{k,i})$ and $\hat{x}_{3j}'(t_{k,i})$ are presented in (15) and (17), and

$$\begin{aligned}&\hat{x}_{2j}(t_{k,i}) = -g(t_{i,k} - t_{j,f_j(t_{i,k})})\\ &+ \gamma_{2j}(t_{j,f_j(t_{i,k})})u_{1j}(t_{j,f_j(t_{i,k})})(t_{i,k} - t_{j,f_j(t_{i,k})}) + x_{2j}(t_{j,f_j(t_{i,k})}),\end{aligned} \qquad (34)$$

$$\begin{aligned}\hat{x}_{4j}(t_{k,i}) =& \gamma_{4j}(t_{j,f_j(t_{i,k})})u_{vj}(t_{j,f_j(t_{i,k})})(t_{i,k} - t_{j,f_j(t_{i,k})})\\ &+ x_{4j}(t_{j,f_j(t_{i,k})}).\end{aligned} \qquad (35)$$

Proof: According to (10), one can rewrite $u_{1i}(t)$ as:

$$u_{1i}(t) = \gamma_{2i}^{-1}(t)\big(g + \sum_{j\in\mathcal{N}_i}(x_{1j}'(t) - x_{1i}'(t)) - x_{2i}(t)\big), \qquad (36)$$

where $x_{1j}'(t)$, $x_{1i}'(t)$, and $x_{2i}(t)$ for $t \in [t_{i,k}\ \ t_{i,k+1})$ are approximated according to (37), (38), and (39) and following the controlled i-th altitude subsystem model presented in (11) as follows:

$$x_{1j}'(t) = x_{1j}'(t_{i,k}) + \int_{t_{i,k}}^{t} x_{2j}(\tau)d\tau \approx \hat{x}_{1j}'(t_{i,k}) + (t - t_{i,k})\hat{x}_{2j}(t_{i,k}), \qquad (37)$$

where $\hat{x}_{1j}'$ is obtained in (15). Besides:

$$x_{1i}'(t) = x_{1i}'(t_{i,k}) + \int_{t_{i,k}}^{t} x_{2i}(\tau)d\tau \approx x_{1i}'(t_{i,k}) + (t - t_{i,k})x_{2i}(t_{i,k}). \qquad (38)$$

And due to (10) and (11):

$$
\begin{aligned}
&x_{2i}(t) = x_{2i}(t_{i,k})\\
&\quad - \sum_{j\in\mathcal{N}_i}\Big(\int\limits_{t_{i,k}}^{t}\big(x'_{1i}(\tau) - x'_{1j}(\tau)\big)d\tau\Big) - \int\limits_{t_{i,k}}^{t} x_{2i}(\tau)d\tau\\
&\approx x_{2i}(t_{i,k}) - (t - t_{i,k})\big(N_i x'_{1i}(t_{i,k}) + x_{2i}(t_{i,k}) - \sum_{j\in\mathcal{N}_i}\hat{x}'_{1j}(t_{i,k})\big).
\end{aligned}
\tag{39}
$$

Now, substituting (37) to (39) into (36) and then using (14) and (18), $\tilde{u}_{1i}(t) = (t - t_{i,k})A_{1i}$ is obtained. Now, in order to have $|\tilde{u}_{1i}| < \zeta_1$, the following inequality should hold:

$$
t < \frac{\zeta_1 + |A_{1i}|t_{i,k}}{|A_{1i}|}. \tag{40}
$$

In a similar way, the scheduling rule is obtained for the translational subsystem. Therefore, according to (13), u_{vi} can be rewritten as follows:

$$
u_{vi}(t) = \gamma_{4i}^{-1}(t)\big(\sum_{j\in\mathcal{N}_i}(x'_{3j}(t) - x'_{3i}(t)) - x_{4i}(t)\big), \tag{41}
$$

where $x'_{3j}(t)$, $x'_{3i}(t)$, and $x_{4i}(t)$ for $t \in [t_{i,k}\ \ t_{i,k+1})$ are approximated by (42) to (44) for the controlled i-th altitude subsystem model presented in (13) and (11):

$$
x'_{3j}(t) = x'_{3j}(t_{i,k}) + \int\limits_{t_{i,k}}^{t} x_{4j}(\tau)d\tau \approx \hat{x}'_{3j}(t_{i,k}) + (t - t_{i,k})\hat{x}_{4j}(t_{i,k}), \tag{42}
$$

where $\hat{x}'_{3j}$ is obtained in (17). In addition:

$$
x'_{3i}(t) = x'_{3i}(t_{i,k}) + \int\limits_{t_{i,k}}^{t} x_{4i}(\tau)d\tau \approx x'_{3i}(t_{i,k}) + (t - t_{i,k})x_{4i}(t_{i,k}). \tag{43}
$$

And due to (12) and (13):

$$
\begin{aligned}
&x_{4i}(t) = x_{4i}(t_{i,k})\\
&\quad - \sum_{j\in\mathcal{N}_i}\Big(\int\limits_{t_{i,k}}^{t}\big(x'_{3i}(\tau) - x'_{3j}(\tau)\big)d\tau\Big) - \int\limits_{t_{i,k}}^{t} x_{4i}(\tau)d\tau\\
&\approx x_{4i}(t_{i,k}) - (t - t_{i,k})\big(N_i x'_{3i}(t_{i,k}) + x_{4i}(t_{i,k}) - \sum_{j\in\mathcal{N}_i}\hat{x}'_{3j}(t_{i,k})\big).
\end{aligned}
\tag{44}
$$

Now, substituting (42) to (44) into (41) and then using (16) and (18), $\tilde{u}_{vi}(t) = (t - t_{i,k})A_{3i}$ is obtained. In order to have $\|\tilde{u}_{vi}\| < \zeta_3$, the following inequality should hold:

$$
t < \frac{\zeta_3 + \|A_{3i}\|t_{i,k}}{\|A_{3i}\|}. \tag{45}
$$

Combining the two scheduling rules (41) and (45), the scheduling rule (31) is concluded. This completes the proof ■.

Remark 9: It is worth noting that approximations in the computations of $u_{1i}(t)$ and $u_{vi}(t)$ in the proof of Theorem 2 can affect $\tilde{u}_{1i}(t)$ and $\tilde{u}_{vi}(t)$, respectively. This approximation is affected by the choice of the scheduling time calculated according to (31) and this, in turn, is influenced by the values of $|A_{1i}|$ and $\|A_{3i}\|$, which can lead to formation producing errors. However, this error can be mitigated by the appropriate selection of the design parameters ζ_1 and ζ_3. For example, by selecting $\zeta_1 \to 0$ and $\zeta_3 \to 0$, $t_{i,k+1} \to t_{i,k}$ according to (31) and this improves the approximation error.

Remark 10: It is worth mentioning that the design parameters ζ_1 and ζ_3 can be selected time varying or any function of time.

Remark 11: Considering the approximations in (15), (17), (37) to (39) and (42) to (44) and comparing with the approximation methods of [19], it is obvious that our method is different in that we do not consider the access of the neighboring agents to the cloud in $[t_{i,k}\ t_{i,k+1})$ and only the last access before $t_{i,k}$ is considered and the approximations are made accordingly. Although this may seem to reduce the accuracy, it leads to a less computational burden. Besides, our formulations especially in computation of scheduling rule, which is more straightforward. Later, in the simulation part, it can be seen that these approximations do not affect the performance of the method.

Corollary 1: **(Non-Zeno Behavior of Scheduling Rule)** Consider the scheduling rule in (31) for the multi-quadcopter system described in Subsection II-D with the control laws (14) and (16), then the sequence of the cloud access update times does not show Zeno behavior.

Proof:. The proof needs to show that there exists a lower bound for the time interval $t_{i,k+1} - t_{i,k}$. This is equivalent to showing that the time intervals $T_{1i} = \frac{\zeta_1 + |A_{1i}|t_{i,k}}{|A_{1i}|} - t_{i,k} = \frac{\zeta_1}{|A_{1i}|}$ and $T_{3i} = \frac{\zeta_3 + \|A_{3i}\|t_{i,k}}{\|A_{3i}\|} - t_{i,k} = \frac{\zeta_3}{\|A_{3i}\|}$ are lower bounded. Since $|x'_{1i}(t)|$ and $|x'_{2i}(t)|$ are bounded, it can be shown that $|A_{1i}| < A_{1max}$ and $\|A_{3i}\| < A_{3max}$, therefore

$$
T_{1i} \geq \frac{\zeta_1}{A_{1max}}, T_{3i} \geq \frac{\zeta_3}{A_{3max}}. \tag{46}
$$

This completes the proof. ■

Remark 12: It is worth mentioning that the attitude controller is designed for the attitude subsystem of each agent separately, and there is no need for data transmission over the graph for this controller. For this purpose a similar method to that presented in [25] can be employed. Toward this, the virtual inputs $u_{xi}(t)$ and $u_{yi}(t)$ are used to generate the reference values for $\theta_i(t)$ and $\phi_i(t)$, i.e. $\theta_{id}(t)$ and $\phi_{id}(t)$ whereUsing these values and a predefined $\psi_{id}(t)$, an attitude controller can be designed for the attitude subsystem by properly designing the input signals $u_{2i}(t)$, $u_{3i}(t)$ and $u_{4i}(t)$ as the torques applied to the body frame in roll, pitch, and yaw directions.

V. Simulation Results

In this section, the efficiency of the proposed controllers is demonstrated through numerical simulations. For this purpose, it is assumed that three quadcopters (with the mass of $m_i = 1.47\text{kg}, i = 1, 2, 3$) communicate with each other through the cloud service in which the 2nd agent sends its information to (and receives the information from) the 1st and the 3rd agents through the cloud as illustrated in Figure 2. The virtual connection graph between agents is also illustrated in Figure 2. The other physical parameters such as the moment of inertia for the quads are chosen similar to the simulation study conducted in [25] (AR Drone Parrot 2.0). The initial conditions

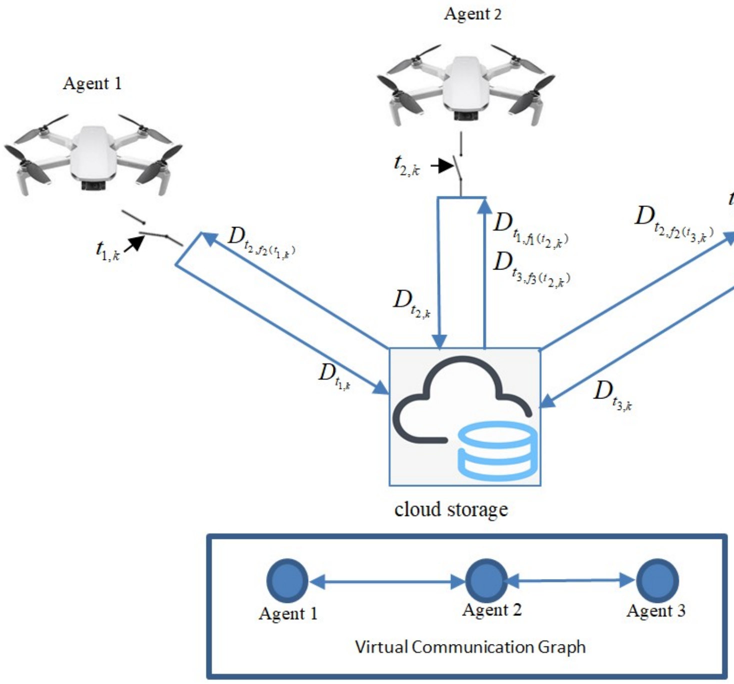

Fig. 2: Example of multi-quad system under cloud access showing the cloud time access and data transmission scenario and the virtual graph between the agents.

chosen for the simulation study are $x_{11}(0) = x_{12}(0) = x_{13}(0) = 0$, $x_{21}(0) = x_{22}(0) = x_{23}(0) = 0$, $x_{31}(0) = [0\ 0]^{\mathrm{T}}$, $x_{32}(0) = [0.2\ 0.2]^{\mathrm{T}}$, $x_{33}(0) = [0.4\ 0.4]^{\mathrm{T}}$, $x_{41}(0) = x_{42}(0) = x_{43}(0) = [0\ \ 0]^{\mathrm{T}}$, $\phi_1(0) = \phi_2(0) = \phi_3(0) = 0$, $\theta_1(0) = \theta_2(0) = \theta_3(0) = 0$, $\psi_1(0) = \psi_2(0) = \psi_3(0) = 0$. Moreover, $b_1 = [0\ 0\ 0]^{\mathrm{T}}$, $b_2 = [0\ 0\ \ -0.5]^{\mathrm{T}}$, $b_3 = [0\ 0\ 0.5]^{\mathrm{T}}$.

A. Evaluation of the Proposed Method

Firstly, we choose $\zeta_1 = 0.03$ and $\zeta_3 = 0.001$. These values are selected according to Remark 8 on selections of ζ_1 and ζ_3 by choosing $\mathcal{X}_1 \approx 0.12$ and $\mathcal{X}_3 \approx 0.062$. Figure 3 shows the positions of agents on the x, y and z axes. It is obvious from the figures that the agents reach average consensus (or practical consensus) plus the bias terms, and therefore the speeds of all agents converge to zero according to Figure 4. The times that the agents are connected to the cloud are presented in Figure 5. Figure 6 depicts the force input signals $u_{1i}, i = 1, 2, 3$ as control input signals and are chosen as piecewise continuous due to discrete connections to the cloud. The torque signals u_{2i} and $u_{3i}, i = 1, 2, 3$ show undesirable fluctuations due to the triggering of the cloud. Such fluctuations are unavoidable. To show that the multi-quadcopter system achieves practical consensus, $\|\xi_1(t)\|$ and $\|\xi_3(t)\|$ are represented against $\mathcal{X}_1$ and $\mathcal{X}_3$, respectively, in Figure 7. This proves that Definition 1 and Theorem 1 are satisfied.

Different values of ζ_1 and ζ_3 (from (21), (22), and (31)) affect cloud access frequency and performance. Table I compares the steady state values of $\|\xi_1(t)\|$ and $\|\xi_3(t)\|$ after 25 seconds of simulation. As ζ_1 and ζ_3 increase, these values increase, as expected from $\mathcal{X}_1$ and $\mathcal{X}_3$ in (21) and (22), respectively. The average value for the cloud access time interval is another parameter. To compute this value, the time intervals between two successive connections to the cloud are computed for all agents, and the average value of all elements for all agents is computed. This value also increases, reducing the number of cloud accesses—an expected and desired outcome. The settling time, calculated from the plots of $\|\xi_1(t)\|$ and $\|\xi_3(t)\|$, also increases with higher ζ_1 and ζ_3. Furthermore, the time averages of the torques and thrust forces increase with increasing ζ_1 and ζ_3

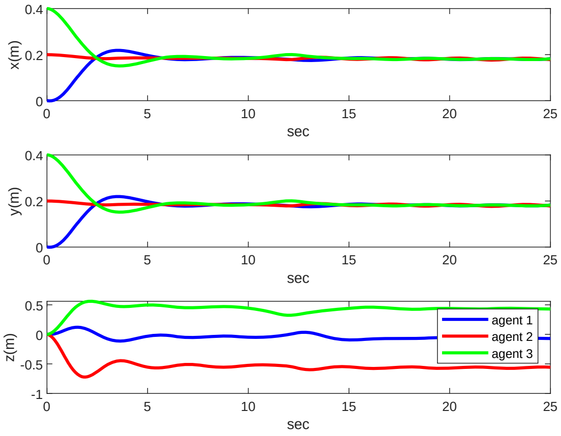

Fig. 3: Position of the agents ($\zeta_1 = 0.03$, $\zeta_3 = 0.001$).

TABLE I: Comparison of different control values as ζ_1 and ζ_3 change and with the extended method of [16].

	$\|\xi_1(25)\|$	$\|\xi_3(25)\|$	Average cloud access time interval (sec)	Settling time 5%(sec)	Average torque (N.m)	Average thrust force (N)	Average number of access to the cloud
$\zeta_1 = 0,\ \zeta_3 = 0$	0	0	0	3.58	0.0264	14.4895	∞
$\zeta_1 = 0.03,\ \zeta_3 = 0.001$	0.02391	0.0047	0.1665	8.3	0.0476	14.4893	167
$\zeta_1 = 0.1,\ \zeta_3 = 0.003$	0.06358	0.0467 (oscillatory)	0.3298	10.01	0.0768	14.4893	87.66
proposed in [19]	–	–	0.1679	4.18	0.0390	14.49	149.6667

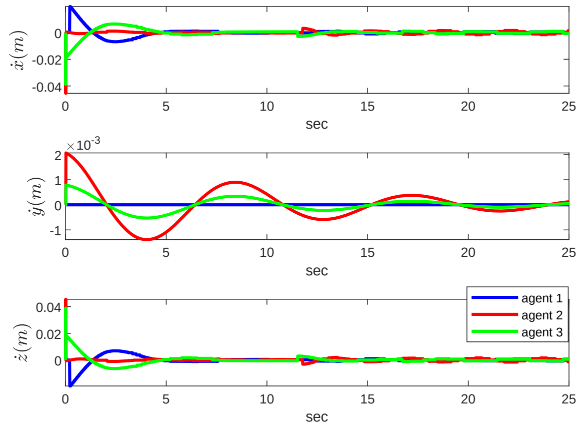

Fig. 4: Translational velocity of the agents ($\zeta_1 = 0.03$, $\zeta_3 = 0.001$).

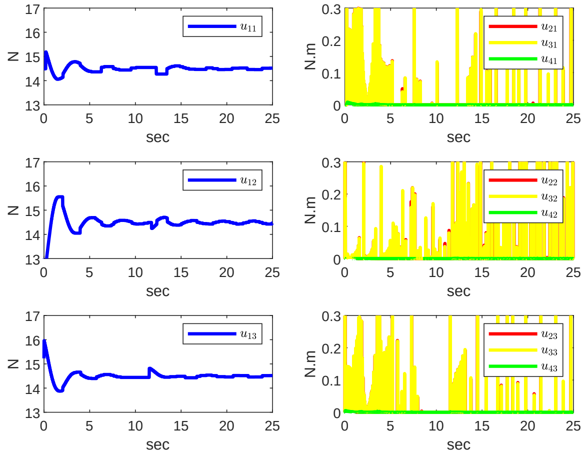

Fig. 6: Control input signals ($\zeta_1 = 0.03$, $\zeta_3 = 0.001$).

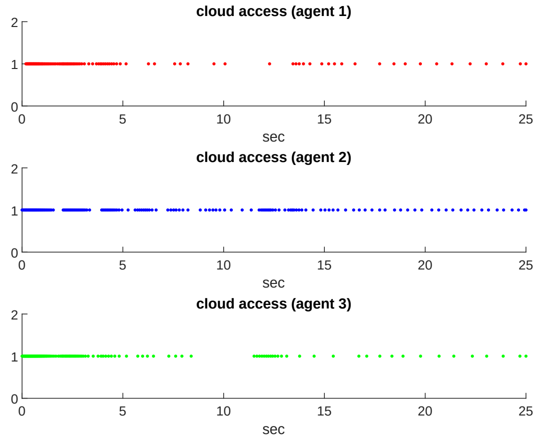

Fig. 5: Access times to the cloud ($\zeta_1 = 0.03$, $\zeta_3 = 0.001$).

B. Comparison with [19] (the Extended Method of [16] for Multi-Quadcopter System)

In [19], the method from [16] for multi-agent formation control with cloud access was extended to multi-quadcopter systems. A comparison of both methods is shown in Table I. Despite different approximations, the access time in this paper should differ significantly, but the performance in terms of cloud access frequency and time intervals is nearly identical. The key difference is that the method in this paper achieves settling times twice as fast. To compute the computational complexity of an algorithm implemented in MATLAB (or any language), we can generally determine the time complexity (how the runtime scales with input size). Since the input sizes of the agents (functions in the MATLAB code) do not change, one can measure the mean value of the actual runtime of all functions (related to the different agents). The results were obtained on an Intel(R) Core(TM) i7-6500U processor, with the method proposed here computing control laws roughly 7 times faster than the one in [19], which is advantageous for large quadcopters groups. The improved computational efficiency is explained in Remark 11. Therefore, the proposed method can be implemented in real time. However, the main issue with [16] and [19] is the consensus filter used. As noted in the Introduction, the consensus-based controller only ensures convergence if the initial velocities of the agents are zero; otherwise, it causes ramp behavior due to changing initial speeds with each cloud connection.

VI. Conclusion

In this paper, the formation producing problem in multi-quadcopter systems under cloud access was studied. For this purpose, first consensus-based formation producing control laws were presented for the altitude subsystem and the translational subsystem with virtual inputs in which the employed consensus control laws guarantee the convergence of the quadcopters' position to the biased average of initial values (asymptotic consensus). Then, the controllers were modified

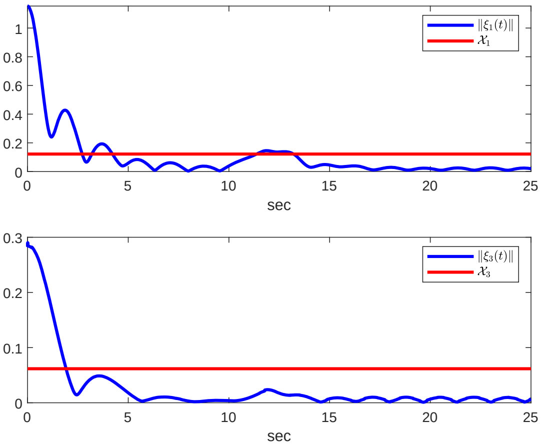

Fig. 7: $\|\xi_1(t)\|$ and $\|\xi_3(t)\|$ against $\mathcal{X}_1$ and $\mathcal{X}_3$ ($\zeta_1 = 0.03$, $\zeta_3 = 0.001$).

to be employed under cloud access where a scheduling rule to communicate with the cloud was designed guaranteeing the practical consensus convergence with a bounded error. The scheduling rule was shown to not exhibit Zeno behavior.

In the simulation results, the performance of the proposed formation producing control laws was evaluated. Toward this, different situations including the continuous inter-agent communication and two different scenarios of cloud access frequency were studied. In addition, the proposed method of this paper was compared with [19].

Although formation control through cloud access results in reducing many communication constraint issues, it can still suffer from some communication constraints, such as packet dropout, cyber attacks and switching connection graphs. In future work, it is suggested to consider communication constraints and cyber attacks under cloud access. Besides, the robustness of the method to parameter uncertainties and disturbances can be considered as the future work.

Appendix I
Proof that F_1 is Hurwitz

Following Assumption 4 assume that the multi-agent system with the connectivity graph $\mathcal{G}$ contains a spanning tree $\mathcal{G}_\mathcal{T}$. In this case, $B_\mathcal{T}$ is a full column rank $N \times (N-1)$ matrix. Let:

$$\lambda\mathbf{I} - F_1 = \begin{bmatrix} \lambda\mathbf{I}_{N-1} & -\mathbf{I}_{N-1} \\ B_\mathcal{T}^\mathrm{T} B T^\mathrm{T} & (\lambda+1)\mathbf{I}_{N-1} \end{bmatrix}. \qquad (47)$$

Remark 13: For a block matrix with the same size square matrix blocks A, B, C and D, $\det \begin{bmatrix} A & B \\ C & D \end{bmatrix} = \det(AD-BC)$ if C and D commute [28].

To prove that F_1 is Hurwitz, first we show $\lambda = 0$ is not an eigenvalue of F_1. For $\lambda = 0$ and following Remark 13, (47) can be simplified to $\det(-F_1) = \det(B_\mathcal{T}^\mathrm{T} B T^\mathrm{T}) = \det\big(B_\mathcal{T}^\mathrm{T} B B^\mathrm{T} B_\mathcal{T} (B_\mathcal{T}^\mathrm{T} B_\mathcal{T})^{-1}\big) \geq \det(B_\mathcal{T}^\mathrm{T} B_\mathcal{T}) + \det\big(B_\mathcal{T}^\mathrm{T} B_\mathcal{C} B_\mathcal{C}^\mathrm{T} B_\mathcal{T}\big) \det\big((B_\mathcal{T}^\mathrm{T} B_\mathcal{T})^{-1}\big)$, where T and $B = [B_\mathcal{T} \;\; B_\mathcal{C}]$ are defined in subsection II-B. Since $B_\mathcal{T}$ is full column rank $\det(B_\mathcal{T}^\mathrm{T} B_\mathcal{T}) > 0$ and $\big(B_\mathcal{T}^\mathrm{T} B_\mathcal{C} B_\mathcal{C}^\mathrm{T} B_\mathcal{T}\big) \geq 0$. This proves that $\lambda = 0$ is not an eigenvalue of F_1. Moreover, using (47) and Remark 13, the characteristic equation of F_1 can be written as:

$$\det(\lambda\mathbf{I} - F_1) = \det\big((\lambda^2 + \lambda)\mathbf{I}_{N-1} + B_\mathcal{T}^\mathrm{T} B T^\mathrm{T}\big). \qquad (48)$$

Remark 14: For any invertible $X_{m\times m}$, $\det(X + AB) = \det(X)\det(\mathbf{I}_n + BX^{-1}A)$ with $A_{m\times n}$ and $B_{n\times m}$ [29].

Following Remark 14, the characteristic equation in (48) can be reformulated as $\det(\lambda\mathbf{I} - F_1) = (\lambda^2+\lambda)^{-1}\det\big((\lambda^2+\lambda)\mathbf{I}_N + \mathcal{L}\big)$ where $\mathcal{L} = BT^\mathrm{T} B_\mathcal{T}^\mathrm{T}$. Therefore, it can be concluded that $\lambda' = \lambda^2 + \lambda$ are eigenvalues of $-\mathcal{L}$ and can be sorted in a set $\{-\lambda'_N, \ldots, -\lambda'_1, 0\}$ so that $-\lambda'_N < \cdots < -\lambda'_1 < 0$. Thus the values of λ have negative real part and this proves that F_1 is Hurwitz.

Appendix II
Proof that F_3 is Hurwitz

We assume

$$\lambda\mathbf{I} - F_3 = \begin{bmatrix} \lambda\mathbf{I}_{(2N-2)\times(2N-2)} & -\mathbf{I}_{2N-2} \\ \big(B_\mathcal{T}^\mathrm{T} B T^\mathrm{T} \otimes \mathrm{I}_2\big) & (\lambda+1)\mathbf{I}_{2N-2} \end{bmatrix}. \qquad (49)$$

Remark 15: Let $A_{n\times n}$ and $B_{m\times m}$, then $\det(A \otimes B) = \det(A)^m \det(B)^n$ [30].

Similar to Appendix I, first we prove that $\lambda = 0$ is not an eigenvalue of F_3. By setting $\lambda = 0$ and applying Remarks 13 and 15 we have: $\det(\lambda\mathbf{I} - F_3)|_{\lambda=0} = \det(-F_3) = \det\Big(\big(B_\mathcal{T}^\mathrm{T} B T^\mathrm{T} \otimes \mathrm{I}_2\big)\Big) = \det(B_\mathcal{T}^\mathrm{T} B T^\mathrm{T})^{N-1}$. As shown in Appendix I $\det(B_\mathcal{T}^\mathrm{T} B T^\mathrm{T}) > 0$, and hence $\lambda = 0$ is not an eigenvalue of F_3. Moreover, using (49) and Remarks 13 and 14, the characteristic equation of F_3 can be written as:

$$\begin{aligned}
&\det(\lambda\mathbf{I} - F_3) \\
&= \det\big((\lambda^2+\lambda)\mathbf{I}_{2N-2} + B_\mathcal{T}^\mathrm{T} B T^\mathrm{T} \otimes \mathrm{I}_2\big) \\
&= \det\big((\lambda^2+\lambda)\mathbf{I}_{2N-2} + (B_\mathcal{T}^\mathrm{T} \otimes \mathrm{I}_2)(BT^\mathrm{T} \otimes \mathrm{I}_2)\big) \\
&= (\lambda^2+\lambda)^{-2}\det\big((\lambda^2+\lambda)\mathbf{I}_N + (BT^\mathrm{T} \otimes \mathrm{I}_2)(B_\mathcal{T}^\mathrm{T} \otimes \mathrm{I}_2)\big) \\
&= (\lambda^2+\lambda)^{-2}\det\big((\lambda^2+\lambda)\mathbf{I}_N + (BT^\mathrm{T} B_\mathcal{T}^\mathrm{T}) \otimes \mathrm{I}_2\big) \\
&= (\lambda^2+\lambda)^{-2}\det\big((\lambda^2+\lambda)\mathbf{I}_N + \mathcal{L} \otimes \mathrm{I}_2\big).
\end{aligned} \qquad (50)$$

Therefore, it can be concluded that $\lambda' = \lambda^2 + \lambda$ are the eigenvalues of $\mathcal{L} \otimes \mathrm{I}_2$ and can be sorted in a set $\{-\lambda'_N, -\lambda'_N, \ldots, -\lambda'_1, -\lambda'_1, 0, 0\}$ so that $-\lambda'_N < \cdots < -\lambda'_1 < 0$. Thus, the values of λ have negative real part and this proves that F_3 is Hurwitz.

Remark 16: If $A_{n\times n}$ and $B_{m\times m}$ with eigenvalues $\lambda_1, \ldots, \lambda_n$ and $\mu_1, \ldots, \mu_m$, respectively, then the eigenvalues of $A \otimes B$ are $\lambda_i\mu_j, i = 1, \ldots, n,\ j = 1, \ldots, m$ [30].

Appendix III
Boundness of $u_{1i}(t)$

We can write (8) as $U_1(t) = \Gamma^{-1}\Big(G - \mathcal{L}X_1\prime(t) - X'_2(t)\Big)$ and by multiplying both sides by $B_\mathcal{T}^\mathrm{T}\Gamma_2$ and replacing $\mathcal{L}$ by $BT^\mathrm{T} B_\mathcal{T}^\mathrm{T}$, we arrive at $B_\mathcal{T}^\mathrm{T}\Gamma_2 U_1(t) = B_\mathcal{T}^\mathrm{T} G - B_\mathcal{T}^\mathrm{T} B T^\mathrm{T} B_\mathcal{T}^\mathrm{T} X_1\prime(t) - B_\mathcal{T}^\mathrm{T} X_2(t) = B_\mathcal{T}^\mathrm{T} G - [B_\mathcal{T}^\mathrm{T} B T^\mathrm{T} \;\; \mathbf{I}]\xi_3(t)$.

Using the definition of vector/matrix norm and applying the triangular inequality yields $\|U_1(t)\| \leq \|G\| + \frac{\|[B_{\mathcal{T}}^{\mathrm{T}} B T^{\mathrm{T}} \ \mathbf{I}]\|}{\|B_{\mathcal{T}}^{\mathrm{T}}\|} \|\xi_1(t)\|$, where $\|\xi_1(t)\|$ is bounded. As a result, it can be concluded that $\|U_1(t)\|$, and hence $u_{1i}(t), i = 1 \dots N$ are bounded.

References

[1] N. Sadeghzadeh-Nokhodberiz, A. Can, R. Stolkin, and A. Montazeri, "Dynamics-based modified fast simultaneous localization and mapping for unmanned aerial vehicles with joint inertial sensor bias and drift estimation," *IEEE Access*, vol. 9, pp. 120 247–120 260, 2021.

[2] N. Sadeghzadeh-Nokhodberiz, M. Iranshahi, and A. Montazeri, "Vision-based particle filtering for quad-copter attitude estimation using multirate delayed measurements," *Frontiers in Robotics and AI*, vol. 10, p. 1090174, 2023.

[3] K. Tiwari and N. Y. Chong, *Multi-robot Exploration for Environmental Monitoring: The Resource Constrained Perspective*. Academic Press, 2019.

[4] N. S. Nokhodberiz, H. Nemati, and A. Montazeri, "Event-triggered based state estimation for autonomous operation of an aerial robotic vehicle," *IFAC-PapersOnLine*, vol. 52, no. 13, pp. 2348–2353, 2019.

[5] N. Sadeghzadeh-Nokhodberiz and N. Meskin, "Protocol-based particle filtering and divergence estimation," *IEEE Systems Journal*, vol. 15, no. 3, pp. 4537–4544, 2020.

[6] Y. Chen, S. Li, Y. Yan, and G. Liu, "Distributed periodic event-triggered consensus of second-order nonlinear multiagent systems with switching topologies," *IEEE Systems Journal*, 2024.

[7] F. Wang, S. He, C. Zhou, Y. Gao, and Q. Zong, "Distributed practical finite-time formation control of quadrotor uavs based on finite-time event-triggered disturbance observer," *IEEE Systems Journal*, 2023.

[8] C. Chen, X. Gao, H. Zhang, W. Zou, and Z. Xiang, "Sampled-data connectivity-preserving consensus for multiple heterogeneous euler-lagrange systems," *IEEE Transactions on Automation Science and Engineering*, 2024.

[9] C. Chen, W. Zou, and Z. Xiang, "Event-triggered connectivity-preserving formation control of heterogeneous multiple usvs," *IEEE Transactions on Systems, Man, and Cybernetics: Systems*, 2024.

[10] Y. Zhou, H. Ge, B. Ma, S. Zhang, and J. Huang, "Collaborative task offloading and resource allocation with hybrid energy supply for uav-assisted multi-clouds," *Journal of Cloud Computing*, vol. 11, no. 1, p. 42, 2022.

[11] J. Wang, C. Jiang, Z. Han, Y. Ren, R. G. Maunder, and L. Hanzo, "Taking drones to the next level: Cooperative distributed unmanned-aerial-vehicular networks for small and mini drones," *IEEE VehIcular Technology Magazine*, vol. 12, no. 3, pp. 73–82, 2017.

[12] W. Ren and Y. Cao, *Distributed coordination of multi-agent networks: emergent problems, models, and issues*. Springer, 2011, vol. 1.

[13] B. Zhu, L. Xie, and D. Han, "Recent developments in control and optimization of swarm systems: A brief survey," in *2016 12th IEEE international conference on control and automation (ICCA)*. IEEE, 2016, pp. 19–24.

[14] Y. Wang, Q. Wu, Y. Wang, and D. Yu, "Consensus algorithm for multiple quadrotor systems under fixed and switching topologies," *Journal of Systems Engineering and Electronics*, vol. 24, no. 5, pp. 818–827, 2013.

[15] A. Can, H. Efstathiades, and A. Montazeri, "Desing of a chattering-free sliding mode control system for robust position control of a quadrotor," in *2020 International Conference Nonlinearity, Information and Robotics (NIR)*, 2020, pp. 1–6.

[16] A. Adaldo, D. Liuzza, D. V. Dimarogonas, and K. H. Johansson, "Cloud-supported formation control of second-order multiagent systems," *IEEE Transactions on Control of Network Systems*, vol. 5, no. 4, pp. 1563–1574, 2017.

[17] W. Ren and E. Atkins, "Distributed multi-vehicle coordinated control via local information exchange," *International Journal of Robust and Nonlinear Control: IFAC-Affiliated Journal*, vol. 17, no. 10-11, pp. 1002–1033, 2007.

[18] A. Adaldo, D. Liuzza, D. V. Dimarogonas, and K. H. Johansson, "Coordination of multi-agent systems with intermittent access to a cloud repository," *Sensing and Control for Autonomous Vehicles: Applications to Land, Water and Air Vehicles*, pp. 453–471, 2017.

[19] N. Sdeghzadeh-Nokhodberiz, M.-R. Ghahramani-Tabrizi, and A. Montazeri, "Formation producing control of multi-quadcopter systems under the cloud access," *IEEE Access*, 2025.

[20] R. O. Saber and R. M. Murray, "Consensus protocols for networks of dynamic agents," in *Proceedings of the 2003 American Control Conference*. IEEE, 2003, pp. 951–956.

[21] N. Biggs, *Algebraic graph theory*. Cambridge university press, 1993, no. 67.

[22] R. Olfati-Saber and J. S. Shamma, "Consensus filters for sensor networks and distributed sensor fusion," in *Proceedings of the 44th IEEE Conference on Decision and Control*. IEEE, 2005, pp. 6698–6703.

[23] Z. Zeng, X. Wang, and Z. Zheng, "Convergence analysis using the edge laplacian: Robust consensus of nonlinear multi-agent systems via iss method," *International Journal of Robust and Nonlinear Control*, vol. 26, no. 5, pp. 1051–1072, 2016.

[24] G. Xie and L. Wang, "Consensus control for a class of networks of dynamic agents," *International Journal of Robust and Nonlinear Control: IFAC-Affiliated Journal*, vol. 17, no. 10-11, pp. 941–959, 2007.

[25] N. Sadeghzadeh-Nokhodberiz and N. Meskin, "Consensus-based distributed formation control of multi-quadcopter systems: Barrier lyapunov function approach," *IEEE Access*, vol. 11, no. -, pp. 142 916–142 930, 2023.

[26] G.-D. Hu and T. Mitsui, "Bounds of the matrix eigenvalues and its exponential by lyapunov equation," *Kybernetika*, vol. 48, no. 5, pp. 865–878, 2012.

[27] H. V. Henderson, F. Pukelsheim, and S. R. Searle, "On the history of the kronecker product," *Linear and Multilinear Algebra*, vol. 14, no. 2, pp. 113–120, 1983.

[28] J. R. Silvester, "Determinants of block matrices," *The Mathematical Gazette*, vol. 84, no. 501, pp. 460–467, 2000.

[29] C. Pozrikidis, *An introduction to grids, graphs, and networks*. Oxford University Press, USA, 2014.

[30] C. F. Van Loan, "The ubiquitous kronecker product," *Journal of computational and applied mathematics*, vol. 123, no. 1-2, pp. 85–100, 2000.

Nargess Sadeghzadeh-Nokhodberiz received the B.Sc. and M.Sc. degree in control engineering from Tehran Polytechnic, Tehran, Iran, in 2006 and 2008, respectively. She received her PhD in Sep. 2014 in Control Engineering from Iran University of Science and Technology, Tehran, Iran, in collaboration with Automation Laboratory of Heidelberg University, Heidelberg, Germany. She was with the Department of Engineering at the Islamic Azad University Central Tehran Branch, Tehran, Iran as an assistant professor from 2015 to 2019. She was as a visiting scholar with the Department of Electrical Engineering at Qatar University, Doha, Qatar in 2016 and with the Department of Engineering at Lancaster University, Lancaster, UK in 2018. Since 2019 she is as an assistant professor with the Department of Electrical and Computer Engineering at Qom University of Technology, Qom, Iran. Her research interest focuses on control systems theory, multi-agent systems, mobile robots localization, mapping and formation control.

Allahyar Montazeri received the B.S. degree in electrical engineering from Tehran University, Tehran, Iran in 2000, and the M.Sc. and Ph.D. degrees in electrical engineering from Iran University of Science and Technology, Tehran, Iran, in 2002, and 2009, respectively. Since 2013, he has been appointed as assistant professor at School of Engineering at Lancaster University, United Kingdom where currently he is working there as an associate professor. Dr. Montazeri is recipient of the European research consortium on informatic and mathematics (ERCIM) and Humboldt research awards in 2010 and 2011, respectively. He is also Fellow of Higher Education Academy. His research is funded by different councils and industries in UK such as Engineering and Physical Research Council, Sellafield Ltd, National Nuclear laboratory, and Nuclear Decommissioning Authority. He is currently Editor-in-Chief of the Journal of Intelligent and Fuzzy Systems, Associate Editor of the Frontiers in Robotics and AI journal, and Topical Advisory Board of Robotics MDPI. He also serves as the member of the IFAC Technical Committees 'Adaptive and Learning Systems' and 'Modelling, Identification, and Signal Processing'.